Proceedings of the 17th World Congress
The International Federation of Automatic Control
Seoul, Korea, July 6-11, 2008

Unified MPC strategy for idle-speed control, vehicle start-up and gearing applied to an Automated Manual Transmission

R. AMARI * **M. ALAMIR,** ** **P. TONA** *

* *IFP Powertrain Engineering, BP3, 69390 Vernaison, France (Tel: +33 4-78-02-26-03; e-mail: {rachid.amari,paolino.tona}@ifp.fr).*
** *Gipsa-Lab/ Control Systems Dept. / Sysco-Group, Rue de la Houille Blanche, Domaine Universitaire, St. Martin d'Hères, France (Tel: +33 4-76-82-63-26, e-mail: mazen.alamir@inpg.fr)*

Abstract: A real-time Model Predictive Control (MPC) is proposed for controlling the behavior of an Automated Manual Transmission (AMT). The underlying formulation shows a unified approach that handles different modes: idle-speed control, vehicle start-up, gearing up and down. Sub-optimal solutions are computed on line using an adaptive reduced dimensional parametrization that is directly linked to the accelerator pedal position. Transmission stability constraints are explicitly handled as well as saturations on the control inputs. The proposed control is tested both in simulation and on line in a city car demonstrator equipped with a natural gas engine.

1. INTRODUCTION

Many technical concepts have been developed in automotive industry for coupling engine shaft to wheels. Manual Transmission (MT) was the earliest development and is now widely used because of its high efficiency, low weight and low cost. In this transmission the gear box ratios are discrete. Any gearing needs a total opening of the transmission : first, the clutch should be opened and then a new gear can be engaged. This operating mode is frequent during congested traffic and any non smooth gearing causes a discomfort for passengers because of induced oscillations. To limit these oscillations, Automated Transmission (AT) was proposed as an alternative solution based on a torque converter and planetary gears or a Continuously Variable Transmission (CVT). The comfort can be improved but fuel consumption and manufacturing cost are increased.

A trade-off between Manual Transmission (MT) and Automatic Transmission (AT) can be achieved by using an Automated Manual Transmission (AMT). The latter operates similarly to a manual transmission except that it does not require direct clutch actuation or gear shifting by the driver (see Fig. 1). Embedded control strategies ensure smooth clutch engagement and gear shifting. Comfort is reduced with respect to automatic transmission since gear shifting cannot be achieved without torque interruption, but it can be acceptable provided that control strategies are able to limit the variation of vehicle acceleration during vehicle start-up and gearshifts. Indeed, another trade-off, with a considerable comfort improvement, can be obtained by introducing a dual clutch system: during gear shifting the engine torque is continuously transmitted by second clutch while the first clutch is operated to engage the new gear. However this solution is not as simple nor as cost effective as standard AMTs.

In Dolcini et al. [2005], optimal control of dry clutch engagement is proposed to improve comfort during vehicle start-up. The clutch engagement starts with an open-loop phase, then the optimization is turned on just at the end of the start-up phase to limit the oscillations of the transmission. In this strategy the engine torque is assumed to be a known disturbance rather than a control input as it is the case in the present work. Moreover, due to the complexity of the control computation, only short prediction horizons (0.5 seconds) can be used.

Linear Quadratic Control is proposed in James and Narasimhamurthi [2006] to control the slipping speed. This optimal control takes into account the slip time, the dissipated power and the slip acceleration in the performance index. To select a particular vehicle launch profile, a look-up table is used. The strategy is proposed for transmissions equipped with medium-duty wet clutches in which the dynamic of clutch torsional spring damping coefficients can be neglected. The application of this control to dry clutches seems to be limited since clutch models are very complex. In Glielmo and Vasca [2000], a Linear Quadratic approach for clutch engagement is proposed by introducing weighting factors for slipping speed and control inputs. Direct real-time implementation of this strategy is difficult because of the high computation time required by the on-line solution of a Riccati differential equation. To cope with this problem, authors underline that it is possible to compute off-line the feedback gains and to find the coefficients of polynomials approximating their time evolution.

In Glielmo et al. [2006] a hierarchical approach is proposed by considering five AMT operating phases, defined according to clutch position (*engaged*, *slipping opening*,*go-to-slipping* and *slipping closing*) and gearbox operation (*synchronization*). In closed-loop control phases, the strat-

978-1-1234-7890-2/08/$20.00 © 2008 IFAC

10.3182/20080706-5-KR-1001.2846

egy uses decoupled PI controllers to control engine and clutch speeds with the assumption that desired speeds are known. Control performances strongly depends on the quality of system decoupling which in turn requires a precise estimation not only of clutch torque but also of engine torque, the latter being seldom available in the case of production engine control systems.

In Bemporad et al. [2001] a model prediction based, piecewise linear feedback control is proposed for clutch engagement control. The associated open-loop optimization problem is solved off-line by multi-parametric programming. During vehicle tests, any new calibration of the control law entails recomputing the corresponding state partitions as well as the associated gains.

The solution proposed in this paper is based on a particular formulation of constrained Model Predictive Control (MPC), an attractive design methodology which enables a unified expression of trade-offs while handling constraints and nonlinearities (Mayne et al. [2000]). In order to yield a real-time implementable scheme, the originally constrained problem (input saturations, final stability condition) is transformed into a parameterized unconstrained quadratic problem. The parametrization of the unconstrained problem involves the prediction horizon that is modified on-line in order to explicitly meet the hard constraints. More precisely, the minimum allowable prediction horizon is directly linked to the accelerator pedal position in order to promote a kind of constrained *transparency* to the driver. An interesting feature of the proposed solution is the unified form that captures the hybrid nature of the problem.

This solution has been developed and tested in the framework of VEHGAN[1], a joint project involving IFP, Gaz de France, Valeo and INRETS[2], partially founded by ADEME[3]. The project investigates the benefits of combining, in a small city car (a MCC `smart`), a dedicated downsized engine (660 cm^3) fuelled with compressed natural gas, with a starter-alternator reversible system based on ultra-capacitors, providing mild-hybrid capabilities. As described in Tona et al. [2007], the `smart` production engine and transmission electronic control units have been replaced by an in-house rapid prototyping powertrain control system, thus making this demonstrator a very flexible test-bed for advanced powertrain control strategies.

The paper is organized as follows: first, the problem is clearly stated (section 2) through the system model, the control objective and the constraints. Section 3 describes the proposed solution. Finally, some validating simulations are proposed in section 4 (using the co-simulation SIMULINK-AMESim environment) as well as preliminary experimental results on the `smart` demo car.

2. PROBLEM STATEMENT

In this section, a simplified system model is first described. Then the control problem is stated together with the associated constraints.

[1] *VÉhicule Hybride au GAz Naturel*, Hybrid CNG Vehicle
[2] The French National Institute For Transport And Safety Research
[3] French Environment and Energy Management Agency

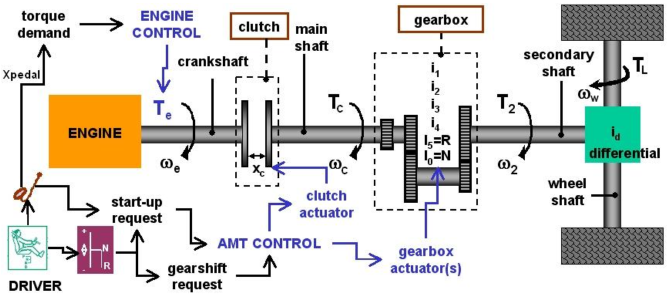

Fig. 1. Automated manual transmission (AMT) system

2.1 System model

During the engagement phase (start-up, gearing), the system can be described by the following simplified model Glielmo et al. [2006] (see Fig. 1):

$$J_e\dot{\omega}_e = T_e - sign(\omega_{sl}) \cdot T_c(x_c) \tag{1a}$$

$$[J_c + J_{eq}(i_g, i_d)]\,\dot{\omega}_c = sign(\omega_{sl}) \cdot T_c(x_c) - \frac{1}{i_g\ i_d}\left[k_{tw}\,\theta_{cw} + \beta_{tw}\left(\frac{\omega_c}{i_g\ i_d} - \omega_w\right)\right] \tag{1b}$$

$$J_w\dot{\omega}_w = k_{tw}\theta_{cw} + \beta_{tw}\left(\frac{\omega_c}{i_g\ i_d} - \omega_w\right) - T_L(\omega_w) \tag{1c}$$

$$\dot{\theta}_{cw} = \frac{\omega_c}{i_g\ i_d} - \omega_w \tag{1d}$$

where:

- J are inertias, T torques, ω and θ angular speeds and positions;
- the subscripts e, c, m, t and w denote engine, clutch, mainshaft, transmission and wheel, respectively;
- x_c is the position of clutch actuator (throwout bearing);
- k and β are elasticity and friction coefficients, respectively;
- i_g is the gear ratio and i_d is the differential ratio;
- J_{eq} is the equivalent inertia of the transmission (mainshaft, synchronizer and driveshaft) given by:
$$J_{eq}(i_g, i_d) = J_m + \frac{1}{i_g^2}\left(J_{S_1} + J_{S_2} + \frac{J_t}{i_d^2}\right)$$
- $\omega_{sl} = \omega_e - \omega_c$ is the slipping speed;
- $\theta_{cw} = \theta_c - \theta_w$
- T_L is the load torque, in general an unknown disturbance, including aerodynamic resistance, tire–road frictions, and road grade.

2.2 Control problem

There are several requirements that contribute to the definition of the control problem. These requirements depend on the vehicle mode (start-up, gearing, idle speed) and have to be fulfilled using the engine torque set-point T_e^{SP} and the clutch torque set-point T_c^{SP}. These set-points are sent to the local low-level controllers.

Control of the slipping speed ω_{sl}

This control is needed in start-up and gearing modes and aims to guarantee a smooth clutch closing at the end of

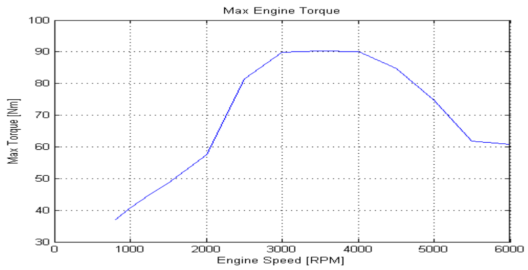

Fig. 2. Maximum engine torque $\mathcal{T}(\omega_e)$ vs engine speed

each transient phase. This can be written in terms of a tracking problem:

$$\omega_{sl}(\cdot) \approx \omega_{sl}^{ref}(\cdot)$$

where ω_{sl}^{ref} is some reference profile to be tracked that is such that the slipping speed smoothly reaches 0 after some transient time t_f. The corresponding transient duration t_f must faithfully reflect the demand expressed by the driver through the accelerator pedal position X_{pedal} (*transparency*).

Control of the engine speed ω_e

This control is needed in the start-up, gearing and idle speed modes. Under these modes, the engine velocity ω_e has to track the following reference:

$$\omega_e^{ref} = \max\{\omega_e^0, \mathcal{T}^{-1}(T_e^d(X_{pedal}, \omega_e))\} \tag{2}$$

where:

- ω_e^0 is the idle speed set-point
- $\mathcal{T}(\omega_e)$ is the maximum torque at speed ω_e as depicted in Fig. 2.
- $T_e^d(X_{pedal}, \omega_e)$ is the desired torque as *interpreted* using the static map shown in Fig. 3.

Equation (2) expresses that the engine speed ω_e is regulated at ω_e^0 unless the desired torque exceeds the maximum torque $\mathcal{T}(\omega_e)$ that can be produced by the engine (see Fig. 2).

Constraints

The control tasks have to be achieved while meeting the following constraints:

- saturation constraints on torques and their variation rates:

$$T_e \in [T_e^{min}, T_e^{max}(\omega_e)] \tag{3}$$
$$T_c \in [T_c^{min}, T_c^{max}(\omega_e)] \tag{4}$$
$$\dot{T}_e \in [\dot{T}_e^{min}, \dot{T}_e^{max}] \tag{5}$$
$$\dot{T}_c \in [\dot{T}_c^{min}, \dot{T}_c^{max}] \tag{6}$$

  where $T_e^{max}(\cdot)$ is shown in Fig. 2. The same curve is used to define T_c^{max} since this corresponds to all realistic value that may be expected for T_c.

- *no-kill* condition on engine speed:

$$\omega_e \geq \omega_e^{min}$$

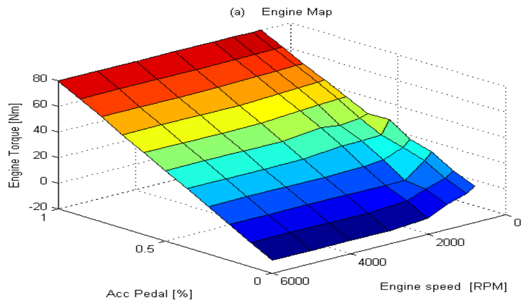

Fig. 3. Demo car pedal torque map $T_e^d(X_{pedal}, \omega_e)$

- *no-lurch* conditions (Garofalo et al. [2002]) on slipping speed:

$$\omega_{sl}(t_f) = 0$$
$$\dot{\omega}_{sl}(t_f) = 0$$

The controller uses measurements of ω_e and ω_c. In particular, the effectively achieved torques T_e and T_c are not directly measured and result from the low-level control loops mentioned above.

3. PROPOSED SOLUTION

3.1 Model reduction

In order to design a real-time implementable MPC, the system model (1) is first simplified as follows:

$$J_e\dot{\omega}_e = u_1 - sign(\omega_{sl}) \cdot u_2 + \delta_e \tag{7a}$$
$$[J_c + J_{eq}(i_g, i_d)]\,\dot{\omega}_c = sign(\omega_{sl}) \cdot u_2 - \delta_c \tag{7b}$$

where

$$u := \begin{pmatrix} T_e^{SP} & T_c^{SP} \end{pmatrix}^T$$

stands for the vector of set-points fed to the local controllers while δ_e and δ_c are used to gather all model mismatches and/or tracking errors including the load torque T_L. The MPC controller described hereafter uses estimations $\hat{\delta}_e$ and $\hat{\delta}_c$ for δ_e and δ_c. These can be obtained through Kalman-like observers based on the measured quantities ω_e, ω_c and u. In the remainder of the paper, the following discrete and compact form is used for (7):

$$\omega^+ = \omega + B(i_g, q_1) \cdot u + G \cdot \delta \tag{8}$$

where $\omega = (\omega_e, \omega_c)^T$ and $q_1 \in \{0, 1\}$ is a binary variable depending on the sign of ω_{sl}. Note that (8) is valid on sampling periods during which $sign(\omega_{sl})$ is constant. This will be enhanced by on-line constraints as explained below (see section 3.3). On the other hand, we are interested in what happens for a given value of i_g describing the present driver demand.

3.2 Basic idea

In this section, the main ideas underlying the structure of the control law are described. The related details are then successively explained.

As in any MPC scheme, the decision variable updated at each decision instant k is the sequence of future actions given by:

$$\tilde{U}(k) = \left(u^T(k), \dots, u^T(k+N_p-1)\right)^T \in \mathcal{U}(k) \subset \mathbb{R}^{2N_p}$$

where N_p is referred to hereafter as the *prediction horizon* while $\mathcal{U}(k)$ defines the admissible set that may depend on the context through the time index k. The sequence $\tilde{U}(k)$ is computed by minimizing some cost function $J_{\nu(k)}(\tilde{U}, \omega(k))$ that depends on the state $\omega(k)$ and a vector of exogenous data $\nu(k)$ that is given by:

$$\nu := \begin{pmatrix} \hat{\delta} \\ N_f^* \\ X_{pedal} \end{pmatrix} \in \mathbb{R}^2 \times \mathbb{N} \tag{9}$$

where $\hat{\delta}$ is the current estimation of $\delta := (\delta_e, \delta_c)$, N_f^* is the launching phase duration index that is a parameter to be updated on line as explained below while X_{pedal} is the accelerator pedal position that is explicitly used in the expression of the cost function in order to enhance the transparency property invoked in the preceding section. The cost function expresses deviation with respect to some desired behavior.

Once some optimal sequence

$$\hat{U} := \left(\hat{u}^T(k), \dots, \hat{u}^T(k+N_p-1)\right)$$

is obtained, the MPC control amounts to apply the first input in the optimal sequence, namely $\hat{u}(k)$ during the sampling period $[k\tau_s, (k+1)\tau_s]$. At the next decision instant $(k+1)\tau_s$, the new cost function $J_{\nu(k+1)}(\tilde{U}, \omega(k+1))$ is used to compute $\hat{u}(k+1)$ and so on.

It goes without saying that solving the constrained optimization problem $\min_{\tilde{U} \in \mathcal{U}(k)} J_\nu(\tilde{U}, \omega)$ on-line would be beyond any standard on-board computational power. The following facts enable a sub-optimal version to be used on-line:

- first, for each value of the parameter N_f^* the cost function J_ν is quadratic in $\tilde{U}$ as shown below;
- the constrained problem $\min_{\tilde{U} \in \mathcal{U}(k)} J_\nu(\tilde{U}, \omega)$ is replaced by the N_f-parameterized unconstrained one given by:

$$\min_{\tilde{U} \in \mathbb{R}^{2N_p}} \left[J_{\nu(k)}(\tilde{U}, \omega(k))\right] \text{ under (3)-(6)} \tag{10}$$

- moreover, it can be shown that there is always a choice of N_f^* such that the solution of (10) lies in the admissible set $\mathcal{U}(k)$.

3.3 Definition of the quadratic cost function J

In a torque-oriented engine control structure, driver's demand is expressed through the accelerator pedal and seen as a torque demand. The key idea is to transform driver's demand into a clutch-closing phase duration $t_f = N_f \cdot \tau_s$ using a look-up table shortly denoted hereafter by:

$$\begin{array}{ccc} [0 \quad 100] & \rightarrow & [t_f^{min} \quad +\infty] \\ X_{Pedal} & \mapsto & t_f = f(X_{Pedal}) \end{array}$$

For this, at each instant k, a reference trajectory for the slipping speed ω_{sl} is defined as follows:

$$\forall i \in \{1, \dots, N_p-1\}$$
$$\omega_{sl}^{ref}(k+i) = \frac{1 - i/N_f^*}{(1+\lambda \cdot i/N_f^*)^2}\omega_{sl}(k) \tag{11}$$

which starts at the present value $\omega_{sl}(k)$ and ends at zero slipping speed after N_f^* sampling periods. The value of the parameter N_f^* is taken to be the closest possible (under saturation constraints) to $N_f = t_f/\tau_s = f(X_{pedal})/\tau_s$. This enables the transparency requirement to be satisfied. As for the constraint $\dot{\omega}_{sl} = 0$, it can be approximately enhanced using high values of λ.

The cost function J is therefore defined by the tracking requirementsspecifications on ω_{sl} and ω_e w.r.t to the reference trajectories given by (11) and (2) respectively. This is shortly written as follows:

$$J_{\nu(k)}(\tilde{U}, \omega(k)) := \sum_{i=1}^{N_p} \left\| \begin{pmatrix} \omega_{sl}(k+i) - \omega_{sl}^{ref}(k+i) \\ \omega_e(k+i) - \omega_e^{ref}(k+i) \end{pmatrix} \right\|_Q^2 \tag{12}$$

where $\omega_{sl}(k+\cdot)$ and $\omega_e(k+\cdot)$ are the predictions based on the initial state $\omega(k)$, using the future candidate sequence $\tilde{U}$ and the estimation $\hat{\delta}$ while the reference trajectories $\omega_{sl}^{ref}(k+\cdot)$ and $\omega_e^{ref}(k+\cdot)$ are computed according to (11) and (2) using the information N_f^* and X_{pedal} included in the exogenous input ν. Note however that while X_{pedal} is imposed by the driver, the value of the horizon N_f^* is still a degree of freedom that is to be tuned.

Now, since the system model (8) is affine in u (under constant sign of ω_{sl}), equation (12) can shortly be written in the following quadratic form:

$$J_{\nu(k)}(\tilde{U}, \omega(k)) = \tilde{U}^T H \tilde{U} + 2\Big[W(N_f^*, \hat{\delta}, X_{pedal}, \omega(k))\Big]\tilde{U}$$

When solving (10), the explicit handling of the inequality constraints (3)-(6) would be computationally demanding for the engine management system. That is why, a sub-optimal solution of the original problem (10) is obtained by tuning the value of the parameter N_f^*. This is done by performing a finite number of computations of the unconstrained optimal solutions:

$$\left\{\hat{U}_N := -H^{-1}W(N, \hat{\delta}, X_{pedal}, \omega(k))\right\}_{N \in \{N_f, \dots\}} \tag{13}$$

for different values of N starting from the minimal value $N_f = f(X_{pedal})/\tau_s$ and using a dichotomy-like iteration in order to fit all the saturation constraints together with the constraint on constant sign of the slipping speed over the prediction horizon, namely:

$$sign\big(\omega_{sl}(k)\big) \cdot \omega_{sl}(k+i) \geq 0$$

What makes such dichotomic solution possible is the fact that high values of N lead to a slow settling time that is likely to correspond to a low torque requirement. On the other hand this would make ω_{sl} approach 0 without sign change since prediction plays the role of a *derivative* term in the controller.

3.4 Idle speed control

In the case of idle speed mode, the same framework is used with the simplest model consisting of equation:

$$J_e \dot{\omega}_e = u_1 + \delta_e$$

and the tracking problem involving only the ω_e-related quadratic terms. Notice that fast action on engine speed through modification of the optimal spark advance is not taken into account directly in the present formulation.

4. VALIDATION

In this section, some simulations as well as preliminary experimental results are given. Simulations are performed using either a reduced model in SIMULINK or an AMESIM simulator (Albrecht et al. [2006]) which provides an accurate description of the relevant interactions and phenomena in the engine and the transmission paths (see Fig. 6). In the AMESIM simulator, a mean-value model (MVEM), driven by air throttle and wastegate positions, injected fuel mass-flow and spark advance, is used for the engine, while the transmission components are chosen to implement the dynamics of the elastic driveline model (1).

Simulations under SIMULINK enable the observer performance in retrieving the value of δ to be illustrated. In all the simulations, the sampling period for MPC control updating is taken equal to $\tau_s = 50\ ms$, while the mean computation time needed to implement the whole control scheme including all the local loops related computations amounts to about $200\mu s$ which is far lower than the actuators basic updating period of $1ms$.

Fig. 4 and 5 show SIMULINK based simulations of the start-up mode respectively with low torque and high torque demands. Recall that the reference trajectory ω_e^{ref} defined by (2) takes into account the need for higher engine speed (Fig. 5.(a)) in presence of high torque demand (Fig. 5.(c)) while for low torque demand, the set-point value of ω_e is almost constant and close to idle speed set-point ($\simeq 1100rpm$) [4].

Note also that the maximum allowable torque T_e is time-varying according to ω_e and that during quite long periods, T_e is saturated. This is due to the very nature of moving horizon technique that enables such behavior even for quadratic unconstrained (but parameter-varying) cost function. This can be seen in the visible coupling between X_{pedal} and horizon length N_f^* (Fig. 5.(c)-(d).

Fig. 7(b) and Fig. 7(a) compare the proposed MPC control to a PI-based strategy presented in (Tona et al. [2007]) and currently implemented on the demo car. The latter controls engine speed through clutch position during vehicle start-up, as depicted in Fig. 8. Contrary to the MPC strategy, the PI-based strategy is unable to perform vehicle start-up without a significant increase of engine speed.

Fig. 9 and 10 show the behavior in co-simulation (model in AMESIM, control in SIMULINK) of the controlled system in the gearing-up and down modes respectively. Note the lower bound 0 on the control variable T_e that makes the settling time in the gearing-up mode slightly higher than that of gearing-down. Note also the discontinuity on ω_c that is due to the engagement of the new gear i_g.

Finally Fig. 11 and 12 show preliminary experimental results in the idle-speed mode. Closed-loop behavior under set-point changes in the desired engine speed ω_e^0 is shown in Fig. 11. Fig. 12 shows a sequence of deactivations/activations triggered by X_{pedal}. When the acceleration pedal is pushed in idle speed mode, an open loop torque is applied following a look-up table. As soon as $X_{pedal} = 0$, the idle speed control described above is fired and ω_e is stabilized at ω_e^0.

[4] The need for this relatively high value is due to CNG engine specificities

5. CONCLUSION

In this paper, a model predictive control is proposed for Automated Manual Transmission systems. The control scheme enables a unified treatment of the idle speed, start-up, gearing-up and down modes. The basic idea is to use a parameterized QP in which the prediction horizon is tuned on-line in order to fit torque saturation constraints. The scheme uses a simplified transmission model and does not assume perfect knowledge of torque values. The control variables are taken to be the set-points of low-level regulation loops and an on-line observer is used to recover the true values of the torques. The proposed scheme has been validated through simulations as well as (partial) tests on a prototype car. Future developments concern the experimental validation of the other vehicle modes, as well as the optimal tuning of controller and observer parameters.

REFERENCES

A. Albrecht, O. Grondin, F. Le Berr, and G. Le Solliec. Towards a stronger simulation support for engine control design: a methodological point of view. In *New Trends in Automotive Powertrain Control and Modelling*, Rueil–Malmaison, Paris, oct 2006.

A. Bemporad, F. Borrelli, L. Glielmo, and F. Vasca. Hybrid control of dry clutch engagement. In *European Control Conference*, Porto, Portugal, oct 2001.

P. Dolcini, C. Canudas de Wit, and H. Bechart. Improved optimal control of dry clutch engagement. In *16th IFAC World Congress*, Prague, Czech Republic, jul 2005.

F. Garofalo, Glielmo L., L. Iannelli, and F. Vasca. Optimal tracking for automotive dry clutch engagement. In *IFAC 15th Triennial Word Congress*, Barcelona, Spain, 2002.

L. Glielmo, L. Iannelli, V. Vacca, and F. Vasca. Gearshift control for automated manual transmissions. *IEEE /ASME Transactions on Mechatronics*, 11(1):17–26,, feb 2006.

L. Glielmo and F. Vasca. Optimal control of dry clutch engagement. In *Transmission and Driveline Symposium, SAE 2000 World Congress*, Detroit, Michigan, USA, mar 2000.

D. James and N. Narasimhamurthi. Plant identification and design of optimal clutch engagement controller. In *SAE Technical Paper Series*, Michigan, USA, Nov 2006.

D. Q. Mayne, J. B. Rawlings, C. V. Rao, and P. O. Scokaert. Constrained model predictive control: Stability and optimality. *Automatica*, 36:789–814, 2000.

P. Tona, Ph. Moulin, S. Venturi, and R. Tilagone. AMT control for a mild-hybrid urban vehicle with a downsized turbo-charged CNG engine. In *SAE Technical Paper Series*, number 2007-01-0286, Detroit, Michigan, U.S.A., apr 2007.

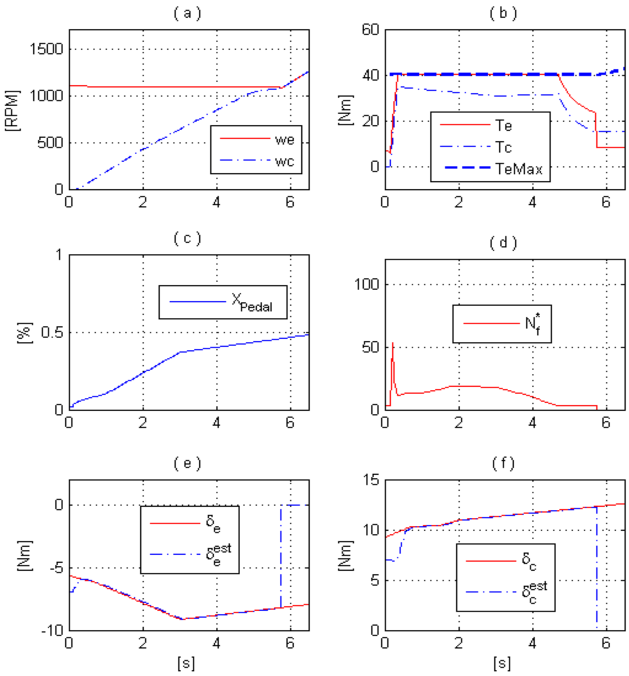

Fig. 4. SIMULINK: Vehicle start-up mode. (Low torque demand)

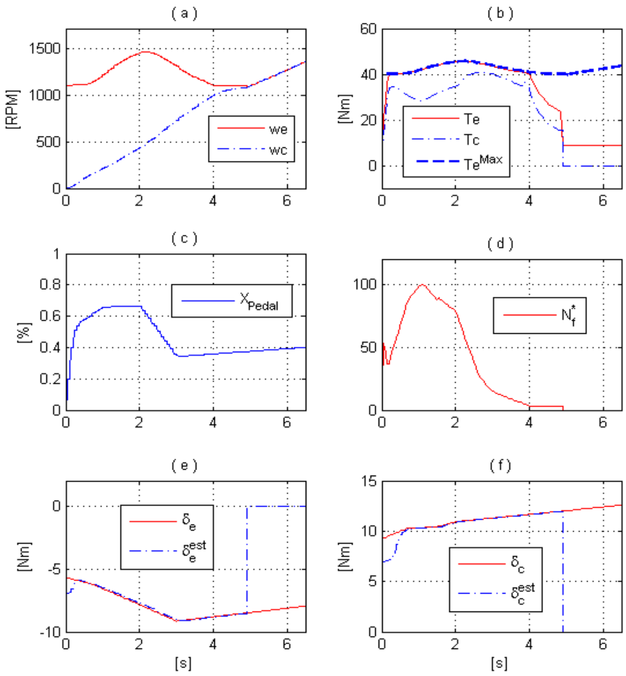

Fig. 5. SIMULINK: Vehicle start-up mode. (High torque demand)

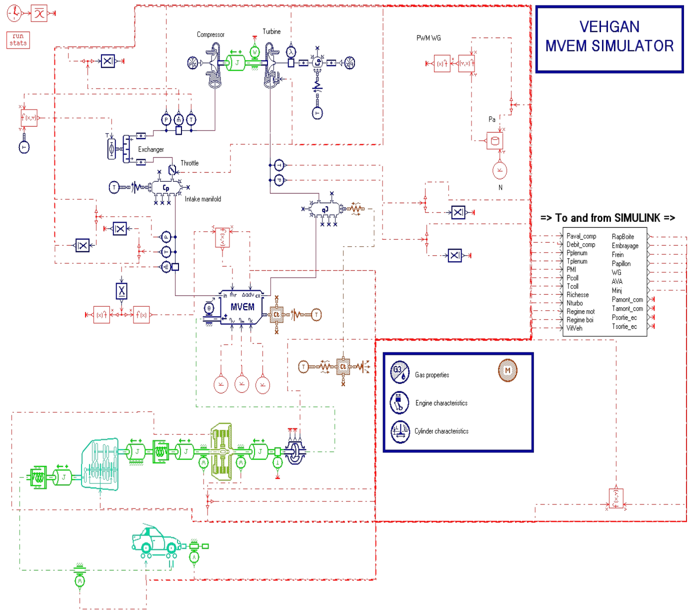

Fig. 6. View of the engine and powertrain model in the AMESim environment

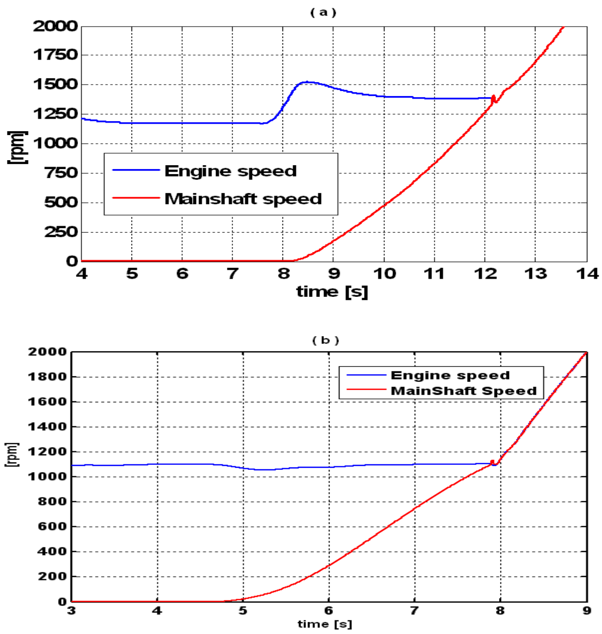

Fig. 7. Co-simulation AMESim/SIMULINK: vehicle start-up mode : comparison between PI (a) & MPC (b) strategies

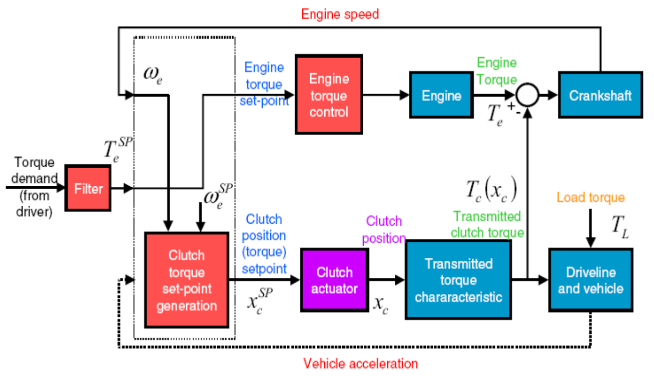

Fig. 8. Control of engine speed through clutch position during vehicle start-up

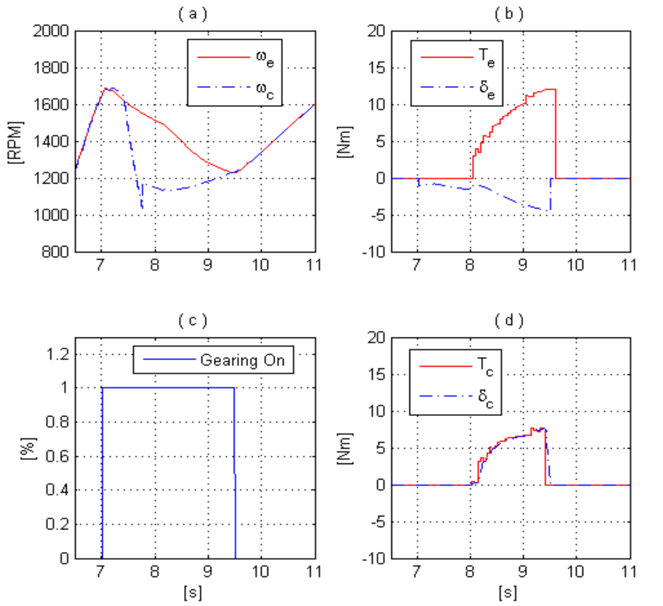

Fig. 9. Co-simulation AMESim/SIMULINK: Vehicle Gearing-up mode (1 → 2)

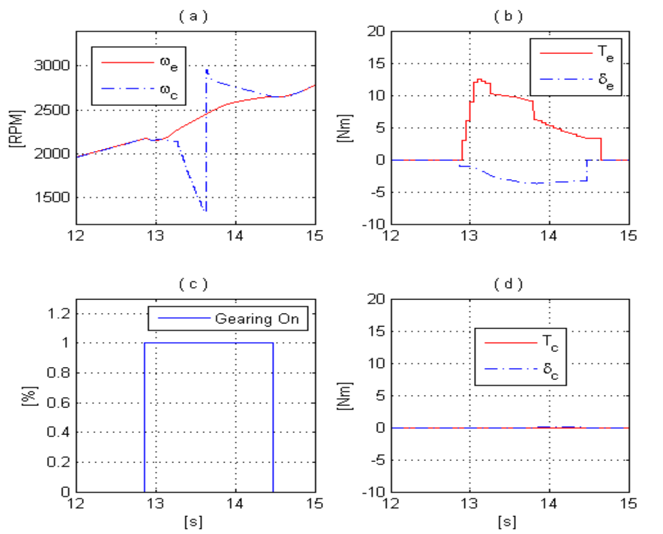

Fig. 10. Co-simulation AMESim/SIMULINK: Vehicle Gearing-down mode (2 → 1)

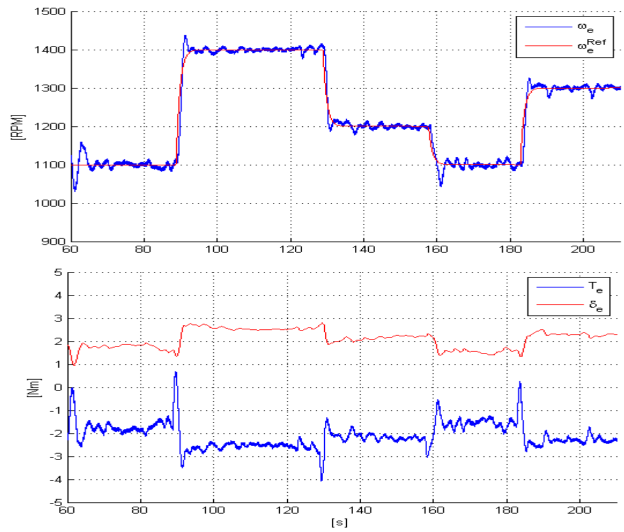

Fig. 11. Experimental results: Idle speed mode. Successive changes in the set-point ω_e^0

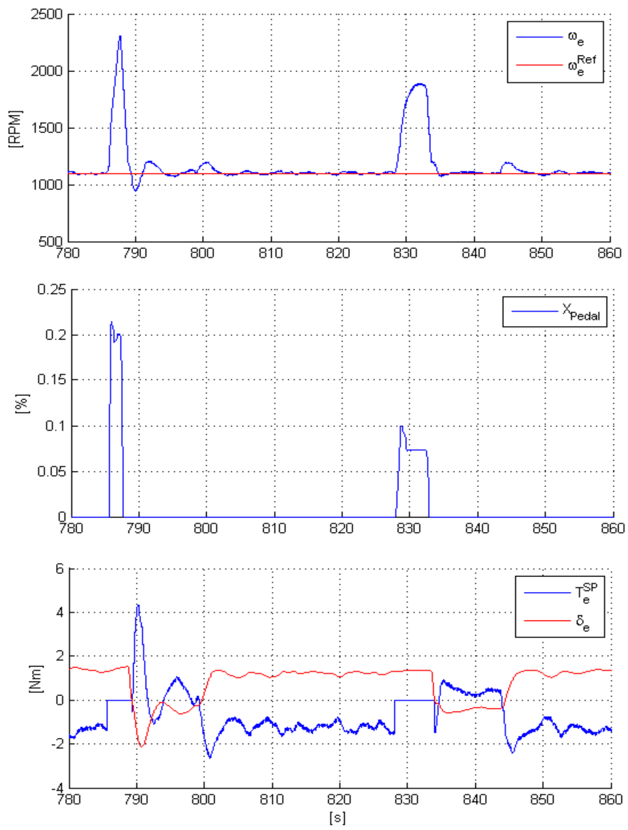

Fig. 12. Experimental results: Idle speed mode. Disturbance rejection. During steps on X_{pedal}, the controller is inactive and open loop torque assignment is used. As soon as $X_{pedal} = 0$, the controller is activated and ω_e is stabilized to ω_e^0.